HHS Public Access

Author manuscript

J Bone Miner Res. Author manuscript; available in PMC 2018 October 01.

Published in final edited form as:

J Bone Miner Res. 2017 October ; 32(10): 2062–2073. doi:10.1002/jbmr.3197.

Therapeutic Effects of FGF23 c-tail Fc in a murine pre-clinical model of X-linked hypophosphatemia via the selective modulation of phosphate reabsorption

Kristen Johnson[1], **Kymberly Levine**[1], **Joseph Sergi**[1], **Jean Chamoun**[1], **Rachel Roach**[1], **Jackie Vekich**[1], **Mike Favis**[1], **Mark Horn**[1], **Xianjun Cao**[1], **Brian Miller**[1], **William Snyder**[1], **Dikran Aivazian**[1], **William Reagan**[3], **Edwin Berryman**[4], **Jennifer Colangelo**[3], **Victoria Markiewicz**[3], **Cedo Bagi**[4], **Thomas P. Brown**[3], **Anthony Coyle**[1], **Moosa Mohammadi**[2], and **Jeanne Magram**[1]

[1]Center for Therapeutic Innovation, Pfizer

[2]Department of Biochemistry & Molecular Pharmacology, New York University School of Medicine

[3]Drug Safety Research and Development, Pfizer

[4]Comparative Medicine, Pfizer

Abstract

Fibroblast growth factor 23 (FGF23) is the causative factor of X-linked hypophosphatemia (XLH), a genetic disorder effecting 1:20,000 that is characterized by excessive phosphate excretion, elevated FGF23 levels and a rickets/osteomalacia phenotype. FGF23 inhibits phosphate reabsorption and suppresses 1α,25-dihydroxyvitamin D (1,25D) biosynthesis, analytes that differentially contribute to bone integrity and deleterious soft tissue mineralization. As inhibition of ligand broadly modulates downstream targets, balancing efficacy and unwanted toxicity is difficult when targeting the FGF23 pathway. We demonstrate that a FGF23 c-tail-Fc fusion molecule selectively modulates the phosphate pathway *in vivo* by competitive antagonism of FGF23 binding to the FGFR/ α klotho receptor complex. Repeated injection of FGF23 c-tail Fc in Hyp mice, a pre-clinical model of XLH, increases cell surface abundance of kidney NaPi transporters, normalizes phosphate excretion and significantly improves bone architecture in the absence of soft tissue mineralization. Repeated injection does not modulate either 1,25D or

Address correspondence to: Kristen Johnson, PhD, Center for Therapeutic Innovation-Pfizer, 450 East 29th Street Suite 403, New York, New York, 20016; Kristen.Johnson@Pfizer.com.

Disclosures:

Kristen Johnson, Kymberly Levine, Joseph Sergi, Jean Chamoun, Rachel Roach, Jackie Vekich, Mike Favis, Mark Horn, Xianjun Cao, Brian Miller, William Snyder, Dikran Aivazian, William Reagan, Edwin Berryman, Jennifer Colangelo, Victoria Markiewicz, Cedo M. Bagi, Thomas P. Brown, Anthony Coyle and Jeanne Magram were all employees of Pfizer at the time this work was performed.

All other authors state that they have no conflicts of interest.

Authors' roles:
Study Design: KJ, JC, MM, JM, AC
Data collection and analysis: KL, JS, KJ, JC, RR, JV, MF, MH, XC, BM, EB, JC
Data interpretation: KJ, JC, WS, DA, CB, TB, VM, WR, CB, MM, JM
Drafting mansuscript: KJ
Editing the manuscript: KL, JS, JC, JM, TB, WR, MM, CB, DA, AC, JM
KJ takes responsibility for the integrity of the manuscript

calcium in a physiologically relevant manner in either a wild-type or disease setting. These data suggest that bone integrity can be improved in models of XLH via the exclusive modulation of phosphate. We posit that the selective modulation of the phosphate pathway will increase the window between efficacy and safety risks, allowing increased efficacy to be achieved in the treatment of this chronic disease.

Keywords

fibroblast growth factor 23; X-linked hypophosphatemia; 1,25D; phosphate; osteomalacia

Introduction

X-linked Hypophosphatemia (XLH) is the most common of the phosphate wasting diseases, affecting approximately 1:20,000 people worldwide (reviewed in (1)). The disease is characterized by low serum phosphate, inappropriately low levels of 1α,25-dihydroxyvitamin D (1,25D) and poor bone mineralization. XLH is typically diagnosed in children upon the appearance of a distinctive bow-legging phenotype, a consequence of the children's 'soft-bones' inability to bear weight as they begin to walk. Other disease manifestations include growth retardation, bone deformation, fractures and bone pain, which continue into adulthood. Disease severity is variable, with some patients requiring multiple invasive surgeries during childhood. Adults suffer from persistent pain, excessive tooth abscesses and calcification of enthese.

Currently, there is no FDA approved standard of care for XLH patients and conventional treatments are cumbersome, not well tolerated, have variable efficacy and harbor significant safety risks. XLH patients rely on phosphate replacement for improved bone mineralization but the persistent phosphate excretion that characterizes the disease makes it challenging to maintain the steady state of serum phosphate necessary to improve and maintain bone integrity. XLH patients receive oral phosphate at regular intervals up to 5 times/day in an attempt to treat their disease but the repetitive nature of phosphate administration leads to hyperparathyroidism (1). Calcitriol, the active form of Vitamin D, is used successfully to combat hyperparathyroidism; however its use increases the potential for soft tissue mineralization, an irreversible condition that can lead to tissue necrosis. As soft tissue mineralization can occur within multiple tissues, including the heart, this safety risk is considered more serious than the hypophosphoteric disease itself. As a consequence, physicians often under dose patients, making it extremely difficult to achieve full efficacy {Carpenter, 2011}.

XLH is defined by a mutation in the phosphate-regulating gene with homologies to endopeptidases on the X chromosome (PHEX) but the causative factor in disease is the upregulation of the endocrine hormone, FGF23 (1). FGF23 functions to decrease serum phosphate and 1,25D levels, minerals crucial for mineralization. FGF23 is secreted by osteoblasts and osteocytes in the bone, ultimately acting on the kidney and parathyroid organs (reviewed by (2). Tissue specificity is achieved by the expression of α-klotho, a membrane protein that acts as a co-receptor to the FGF receptor complex through which

FGF23 signals. Mechanistically, FGF23 regulates phosphate by downregulation of the sodium phosphate (NaPi) transporters in the kidney (3, 4), thereby increasing phosphate excretion. Repression of 1,25D is achieved via modulation of enzymes responsible for the biosynthesis and degradation of Vitamin D (5–9). FGF23 also suppresses parathyroid hormone (PTH), though the mechanisms by which this occurs remain poorly understood (2).

FGF23 is known to be cleaved *in vivo*, resulting in the generation of a C-terminal (c-tail) and an N-terminal fragment (9–11). The c-tail peptide retains the ability to bind to the FGFR1c/α-klotho complex but, in contrast to the full length protein, does not induce signaling (12). Thus cleavage of FGF23 not only inactivates the protein but creates a naturally occurring competitive antagonist. The Mohammadi lab has shown that exogenous delivery of the FGF23 c-tail to rats and mice increases serum phosphate levels *in vivo* (12), raising the possibility that it could be used as a therapeutic in phosphate wasting diseases. However, the half-life of the 72aa c-tail peptide was prohibitively short with an estimated half-life of 10 minutes resulting in a return of phosphate levels to baseline 2 hrs post dosing and prohibiting the assessment of a long-term impact on bone.

We generated a FGF23 c-tail Fc fusion in order to increase the half-life of the FGF23 c-tail peptide and explore the therapeutic potential of this molecule in a pre-clinical mouse model of XLH. We found that treatment of Hyp mice (a mouse model that harbors a mutation in the PHEX gene and mimics human disease) with the FGF23 c-tail Fc over 7 weeks is sufficient to cause dose responsive improvement in bone quality with no evidence of soft tissue mineralization. Interestingly, our molecule preferentially inhibits the phosphate pathway in the absence of 1,25D modulation *in vivo*, regardless of whether the animals are wild-type or diseased. As noted above in the current treatment paradigm, phosphate elevation is associated with bone improvement while elevated 1.25D can increase the risk of soft tissue mineralization. Thus, the unique ability of FGF23 c-tail Fc to preferentially modulate the phosphate pathway in the absence of 1.25D elevation, makes this molecule ideal for use as a new therapeutic in the treatment of XLH, with the potential to significantly improve bone formation in XLH patients with limited safety concerns.

Materials and Methods

Production of recombinant mouse and human FGF23 c-tail Fc constructs and synthetic peptide construct

72aa human FGF23 c-tail peptide (aa 180–251) was synthesized by and resuspended in PBS. The mouse and human Fc-FGF23 fusion protein coding sequences were designed to contain a leader peptide, the hinge and Fc portion of human or mouse IgG1, mutations in the Fc domain that eliminate Fc binding to Fcγ receptors, a single GGGGS linker, and the C-terminal 72 amino acids of human or murine FGF23. The sequences were constructed as syngenes by a commercial vendor (Genewiz, South Plainfield NJ) and recloned into a proprietary mammalian expression vector. The mouse fusion protein was produced by large scale transient transfections using the human embryonic kidney cell line HEK293 using the FreeStyle 293 family of cells, reagents and media (Life Technologies) as per manufacturers' protocols. Murine FGF23-Fc was purified by Protein A affinity (MabSelect SuRe, GE Healthcare, 17–5438) and preparative SEC (Superdex 200pg, GE, 28–9893)

chromatography. The final pool was formulated at approximately 5 mg/ml in 20 mM Hepes, 150 mM NaCl, pH 7.5. The human FGF23 fusion protein construct was transfected into a proprietary CHO cell line and a stable pool of transfectants was selected. After selection, the transfected pool was scaled to 1L at an initial density of 1E6/ml and a production run was initiated. Use of a daily feed schedule enabled production runs of 14–16 days, with typical fusion protein titers of 6–900 mg/L. The supernatants were harvested by centrifugation and sterile filtered before purification. Human FGF23-Fc was purified by Protein A affinity (MabSelect SuRe, GE Healthcare, 17–5438) and ceramic hydroxyapatite (Macroprep CHT Type II, 40 μm, BioRad, 157–4000) chromatography. Preliminary formulation studies were performed at 5 mg/ml and 50–65 mg/ml in HBS (20 mM Hepes, 150 mM NaCl, pH 7.5) and TMS buffer (1.2 mg/ml Tris, 40 mg/ml mannitol, 10 mg/ml sucrose, pH 7.5). The material was most stable in TMS buffer when concentrated to 50 mg/ml. All lots of human and mouse FGF23-Fc were characterized by UV absorbance, SDS-PAGE, Analytical SEC, and endotoxin level. All preparations showed >95% purity by SDS-PAGE and analytical SEC, and endotoxin levels below 1 EU/mg.

Stable cell line generation

Plasmid construction for protein expression of Klotho were made by GenScript. Protein was cloned into the pQCXIN vector (Clontech).

Stable cell lines were generated through retroviral transfection. HEK293T (ATCC) cells were plated at 2E06 cells in 10cm dishes in DMEM (CellGro) with 10% HI FBS and cultured overnight. The following day HEK293T cells were transfected with 5ug of pCL-10A1 retrovirus packaging vector (NovusBio), 5ug plasmid DNA, and Lipofectamine 2000 (Life Technologies). The following day HEK293 and HEK293 α-Klotho cells were plated in 6-well plates (Corning) and cultured overnight. On day 4, HEK293 cells and HEK293 α-Klotho cells were infected with retrovirus containing the gene of interest with 7.5ug/mL of Polybrene. After 48hours cells were passaged as normal with appropriate antibiotic selection reagents.

A lentiviral GreenFire1 pGF1-EGR reporter vector (System Biosciences) expressing destabilized copGFP reporter and firefly luciferase under EGR response elements, a minimal CMV promoter, and the puromycin resistance gene under the control of the EF1 alpha promoter was transfected into HEK293 and HEK293 alpha-Klotho cells. After 48hours cells were negatively selected for and sorted on the FACSAria III (BD Biosciences). Cells were allowed to recover and were expanded. The population of cells was then treated with 200nM TPA (12-O-Tetradecanohylphorbol-13-Acetate Cell Signaling) for 30-minutes. Cells were positively selected for and sorted on the FACSAria III. Cells were then maintained as stated above.

Cell culture

HEK293, a human embryonic kidney cell line, was obtained from the American Type Culture Collection (ATCC) and cultured in Eagle’s Minimum Essential Medium (Corning Cell Gro) containing 10% heat-inactivated fetal bovine serum (HI FBS Life Technologies Gibco). Cells were maintained under standard growth conditions. Cells stably expressing α-

Klotho were selected and maintained in 1.2mg/mL Geneticin (Life Technologies). Cells stably expressing α-Klotho and Egr1 reporter were selected and maintained in 1.2mg/mL G419 (α-Klotho) and 6ug/mL puromycin (Life Technologies). Cells were cultured and split every 72-hours at 1.3×10^6 cells in 20mL of media in a T75 flask.

Animals

Female *Phex*$^{Hyp\text{-}2J}$ mice naïve to any previous treatments were obtained by superovulation of C57BL/6J female mice that were fertilized with sperm from a male *Phex*$^{Hyp\text{-}2J}$ at Jackson Laboratory (Bar Harbor, ME, USA). C57BL/6J age matched naïve mice were supplied by Jackson Laboratory. 6–9 week old Wistar Han IGS rats were purchased from Charles River. Mice were housed 2–3 per cage; rats were housed individually. All rodents were fed a certified rodent diet 5002 (PMI Feeds, Inc) and municipal drinking water ad libitum. All procedures performed on animals in this study were in accordance with established guidelines and regulations, and were reviewed and approved by the Pfizer (or other) Institutional Animal Care and Use Committee. Pfizer animal care facilities that supported this work are fully accredited by AAALAC International.

Cellular reporter assay

HEK293 α-Klotho cells transfected with the Egr-1 reporter were plated in triplicate at 10,000cells/well in 96-well, Poly-D-lysine clear well flat bottom plates (BD Biosciences). Cells were cultured overnight at 37°C in 5%CO_2. On the following day cells were pre-treated with serially diluted amounts of human FGF23 c-tail Fc for 30 minutes. Cells were then treated with 63pM recombinant human carrier-free FGF23 (R&D Systems) for an additional 3 hours. Luciferase expression was quantitated using Steady-Glo Luciferase reagent (Promega) and measured on an Envision (Perkin-Elmer). Data was analyzed and IC50 values were calculated using a 4-parameter variable slope non-linear regression analysis on GraphPad Prism software.

Competitive Binding Assay

HEK93 α-klotho cells engineered and grown as stated above were grown in T75 flasks and removed from flasks using Cell dissociation buffer (Gibco Cat#13151-014) for 3–5min. Cells were counted and placed in 3% BSA/1× PBS blocking buffer (Sigma - Albumin Bovine Fraction V 7.5% solution Cat# A8412) for 1 hour on ice @ 0.2×10^6 cells per 200uL for each condition. A dose response of human FGF23 c-tail Fc peptide was added for a 15 minute pre-treatment on ice to each condition. Human FGF23 protein was then added for one hour on ice at a single dose of 0.47ug/mL (EC80) to each Fc dose and alone. Cells were washed with 400uL cold 0.5% BSA-PBS buffer once and then 200uL cold 0.5% BSA-PBS buffer two additional times. Cells were centrifuged at 1100rpm to pellet the cells after each wash. Anti-HIS mouse mAb (GenScript Cat#A00186-100) was added alone and to each condition at 0.2ug/200uL in 3% BSA-PBS solution for one hour on ice. Cells were then washed as previously described. Anti-mouse PE secondary antibody (Jackson ImmunoResearch Cat# 715-116-150) was then added at 1:200 in 3% BSA-PBS solution alone, with primary antibody, and at each condition and incubated for 45 minutes on ice. Cells were then washed as previously described. Cells were then resuspended in 200uL of 0.5% BSA-PBS and read on the MACSQuant flow cytometer from Miltenyi Biotech.

Short term study in wild type rats

Human FGF23 c-tail Fc was administered into 6–9 week old Wistar Han IGS rats by either subcutaneous injection (10mg/kg N=5 rats; or 30mg/kg N=5 rats) or IV administration (100mg/kg N=5 rats). As a control group a solution of 1.2 mg/mL Tris, 40 mg/mL mannitol, 10 mg/mL sucrose (pH 7.5) was given (N=5 rats). Doses of FGF23 c-tail Fc were given twice weekly by SC injection on Days 1, 4, 8, 11 and 14. The 100 mg/kg dose was given on the same days. The control group was given an intravenous dose followed by a subcutaneous dose. Clinical chemistry parameters were evaluated in samples collected at necropsy on Day 15. The animals were fasted overnight prior to blood collection.

Multi Dose Study in Hyp Mice

On Day 0 of the study murine FGF23 c-tail Fc or phosphate buffered saline (vehicle control) was injected subcutaneously into 5 week old female *Phex*$^{Hyp\text{-}2J}$ mice (0 mg/kg N=44 mice; 3 mg/kg N=10 mice; 10 mg/kg N=15 mice). Additional C57BL/6J age matched female mice were injected on Day 0 with phosphate buffered saline as a second control (N=39 mice). Mice were dosed twice a week until 12 weeks of age (D51). Animals were euthanized on D52. Terminal bleeds were taken by cardiac puncture. Right kidney was collected at necropsy, flash frozen in liquid nitrogen and used to isolate total RNA using Trizol (Invitrogen) using the manufacturer's protocol. Mice were subject to imaging on Day 1 (pretreatment) and 50 (week 8) using a Piximus, automated densitometer. Bone Mineral Density, and fat and lean body composition were assessed. Following necropsy, the right hock and the left kidney were x-rayed using a MX-20 Digital radiography system (Faxitron X-ray LLC, Wheeling IL) and Micro-Computed Tomography (Micro-CT) was conducted on the right femur to measure bone integrity.

Serum and Urine Chemical Parameters

Phosphate, Calcium and Creatinine were measured in serum and/or urine using a Siemen's 1800 Clinical Chemical Analyzer. Quantitation of 1a,25-dihydroxyvitamindihydroxyvitamin D3 [1,25$(OH)_2D_3$] was performed using a UPLC/MS/MS method similar to the method for the quantitation of the inactive form 1α,25-dihydroxyvitamin D_2 was not assessed due to the fact that feed used was only supplemented with the D_3 forms of the vitamin, so D_2 levels were not measurable. Urine samples were collected from group housed non-fasted animals following an overnight collection. Fractional excretion of urine phosphate was calculated to determine the total amount of phosphate excreted. Prior to dose initiation, a group of *Phex*$^{Hyp\text{-}2J}$ or C57BL/6J age matched mice were bled terminally for serum chemistry.

Renal expression of NaPi2A

The right kidney was collected at necropsy, flash frozen in liquid nitrogen, pulverized and total RNA was extracted using Trizol (Invitrogen). 1ug of RNA was used to generate cDNA using random hexamers as per protocol of Invitrogen Superscript Vilo kit. NaPi2A expression was assessed using Invitrogen Taqman probe Slc34a1 (Mn00441450), after normalization to the housing keeping gene B2-microglobulin.

Bone Imaging and Histology

A Piximus, automated densitometer was used to measure Bone Mineral Density (BMD), Bone Mineral Content (BMC) and Bone Mineral Area (BMA), Total Area (T.A.), Total Tissue Mass (TTM) and the percent fat tissue. Micro-Computed Tomography (μCT) evaluation of bone mass, structure and BMD was conducted on the right femur collected at scheduled necropsy. After dissection, the right femur was gently cleaned of soft tissues with a scalpel blade. All bone samples were stored in 10% buffered formalin for a minimum of 48 hours and then transferred to 70% ethanol. μCT analysis was performed on the hock and the cancellous bone on distal femoral metaphyses utilizing a *viva* μCT-40® computed tomography system (Scanco Medical, Bassersdorf, Switzerland). The hind leg was positioned horizontally in a 21 mm holder, with the knee positioned vertically. Using a scout image for reference, a 5mm ROI was identified to include the distal tibia and hock joint. The distal femur sample was oriented horizontally in a 16.5 mm sample holder with the epiphyseal head facing outward. A control file, or measurement protocol, was created to define scanning parameters such as source energy, sample size and image resolution desired. Parameters selected for this study included a source voltage of 55 kV and electric current strength (SI) of 109 μA to obtain the best contrast between bone and soft tissues. The sample area selected for three-dimensional structural analysis of cancellous bone was a 2.0 mm length of the metaphyseal secondary spongiosa, originating 0.5 mm below the epiphyseal growth plate and extending cranially.

To label the newly mineralized bone surfaces, 3 mice from each group received calcein (C-0875, Sigma) and alizarin red S (A-5533, Sigma) at 10 and 3 days, respectively, prior to euthanasia. Calcein was dissolved in 2% sodium bicarbonate/0.9% saline at 10 mg/kg and alizarine in sterile water at 30 mg/mL. Both were dosed at 1 mL/kg as intraperitoneal injections. Undemineralized right tibias were embedded in methylmethacrylate and cut into 8 μm-thick cross sections using a polycut sliding microtome (Leica Biosystems, Nussloch, Germany). Poor mineralization and labeling in *Hyp* mice prevented extensive histomorphometruic analysis. Therefore, the labeling with fluorescent biomarkers was used to demonstrate difference in active mineralization between control WT mice and *Hyp* mice dosed with vehicle and FGF23 c-tail Fc.

Statistics

Statistical tests were conducted at the 5% and 1% significance levels. While all in vivo studies consisted of 3–10 animals per group, several parameters (such as FEPHOS and FECA) required pooling of samples, thus prohibiting statistical analysis. Animal numbers and requirement for pooled samples are strictly documented within the text and figure legends. . Analyses of clinical chemistry, urine and biomarker parameters were done on measurements collected for each animal at the scheduled sampling times. A nonparametric (rank-transform) one way analysis of variance (ANOVA) on groups were conducted, with two-sided trend tests conducted and two-sided pairwise comparisons to the Hyp control group. Average ranks are assigned to ties. The trend tests were performed sequentially using linear contrasts and the pairwise comparisons being done using Dunnett’s test.

For sequential trend tests on bone, if the initial test with all groups included in the trend analysis was significant (trend p-value ≤ 0.05), then it was concluded that the “highest” dose group was different from the “lowest” dose group, and a subsequent trend test is performed on all groups except the “highest” dose group. Testing continued in this manner until a non-significant result was obtained or the test was performed on only the two "lowest" dose groups. All subsequent trend tests were one-sided in the direction suggested by the data in the initial test. As noted within the text, statistical significance does not necessarily represent a change that is biologically significant.

Results

Human 72aa FGF23 C-tail Fc fusion has an inhibitory potency similar to the human 72aa FGF23 C-tail peptide

The 72aa FGF23 C-tail peptide has been shown to inhibit FGF23 mediated activation of the MAPK pathway *in vitro* (12). Additionally, inhibition of MAPK in Hyp mice *in vivo* modulates phosphate and 1,25D and improves bone mineralization, providing evidence that MAPK is a physiologically relevant pathway in FGF23 mediated hypophosphatemia (13). In order to determine whether half-life extension engineering of the 72aa FGF23 c-tail compromised the potency of the peptide, we compared the ability of the FGF23 c-tail peptide and the FGF23 c-tail Fc to inhibit FGF23 mediated induction of Egr1, a transcription factor whose activity is upregulated downstream of the MAPK pathway following stimulation. Specifically, we pre-treated HEK293 cells that were engineered to stably express both α-klotho and an Egr1 luciferase reporter with increasing amounts of either FGF23 c-tail peptide or FGF23 c-tail Fc prior to stimulating cells with a sub-saturating amount of recombinant FGF23 and assessed luciferase reporter activity. This study took advantage of endogeneous expression of FGFRs in HEK293 cells. As shown in Figure 1A, both molecules inhibited luciferase activity in a dose dependent manner, generating IC50s in the range of 200 nM. Therefore, c-terminal fusion of the FGF23 c-tail to a human Fc molecule devoid of effector function did not compromise functional potency of the molecule.

In order to establish that the mechanism of action for competitive inhibition was happening at the level of receptor binding, we performed cellular competitive binding assays using flow cytometry. In this assay, binding of a sub-saturating dose of FGF23 to HEK293-klotho was assessed in the absence or presence of increasing amounts of the FGF23 c-tail Fc. The potency of inhibitory binding was quantitated by plotting the mean florescence intensity (MFI) generated at each concentration of FGF23 c-tail Fc, allowing the generation of an IC50. We noted that HEK293 cells express FGFR1, FGFR3 and FGFR4, each of which can complex with α-klotho (14). These data demonstrated that the FGF23 c-tail inhibited FGF23 at the level of receptor binding and quantitatively demonstrated the FGF23 c-tail Fc has comparable inhibitory binding potency to the FGF23 c-tail peptide, a molecule that has the ability to modulate phosphate *in vivo* (Figure 1B).

Human FGF23 C-tail Fc modulates serum phosphate but not 1,25D in wild-type rats

Previous studies showed exogenous delivery of the FGF23 c-tail to rats and mice increased serum phosphate levels *in vivo* (12). We wished to extend these studies to the FGF23 c-tail Fc and include analysis of 1,25D, an additional target of FGF23. FGF23 c-tail Fc was injected subcutaneously into healthy rats twice a week over 2 weeks at 10, 30 and 100mg/kg, assessing both phosphate and 1,25D levels in the serum on day 15, 24 hrs after the final dose was administered. As seen in Figure 2, serum phosphate was significantly modulated in a dose dependent manner while 1,25D levels did not change at any of the administered dose levels. Hence, FGF23 c-tail Fc molecule appears to selectively modulate phosphate pathways *in vivo*.

Murine FGF23 c-tail Fc modulates phosphate levels in Hyp mice via regulation of NaPi2A expression

The above studies demonstrated that the FGF23 c-tail modulated the phosphate pathway in a wild-type setting without affecting 1,25D levels. However, it remains unclear whether the selective modulation of the phosphate pathway would be recapitulated in the disease setting and if so whether modulation of phosphate alone would be sufficient to improve bone mineralization. In order to test this, we undertook a 7 week study in Hyp mice to assess whether treatment with the FGF23 c-tail Fc improved hypophosphatemia and bone integrity without causing soft tissue mineralization. As in human disease, Hyp mice have elevated levels of FGF23 due to a mutation in PHEX, an endopetidase expressed in the bone (15, 16). For these studies mice were injected twice a week subcutaneously between the ages of 5–12 weeks, the active longitudinal bone growth phase of these mice. Serum/urine chemistry, bone integrity and soft-tissue mineralization were assessed at the end of the study. Of note, though the human molecule does cross react in mice, a surrogate molecule was used for these studies in order to prevent formation of antidrug antibody. While FGF receptors and α-klotho share a high homology between human and mouse proteins (over 86% in all cases), FGF23 homology is 72% between human and mouse, with homology of the 72aa FGF23 c-tail falling to 64%. As described within the materials and methods, both the human molecule and the murine surrogate were made with an effectorless IgG1 Fc. Finally, we verified that the surrogate molecule was shown to have a similar potency to the human molecule *in vitro* when using an all murine system vs an all human system respectively (data not shown).

Consistent with the rat study, serum phosphate showed a trend towards elevation after treatment, 24 hrs post dose at day 52 (Figure 3A) though these changes were not statistically significant (see discussion). Of note, serum phosphate was only modulated at the highest dose and did not reach levels seen in wild-type animals. Interestingly, phosphate excretion was dose responsive and normalization occurred in the 10mg/kg treatment group (Figure 3B). Unfortunately, the necessity to pool urine samples resulted in 2 data points/10 animals/ treatment group, thus prohibiting statistical analysis. . Together, these data show that the FGF23 c-tail Fc impacted phosphate levels in diseased mice and affected phosphate excretion to a greater extent than serum phosphate (at this time point).

FGF23 modulates phosphate levels via downregulation of the sodium transporters located within the kidney; thus increasing phosphate excretion (3, 4). In order to verify the

mechanism of action by which the FGF23 c-tail Fc modulates phosphate levels, we assessed NaPi2a expression relative to B2 microglobulin from total kidney RNA in animals at the end of the study using QPCR. As shown in Figure 3C, a dose dependent increase in NaPi2a expression was found after treatment with the FGF23 c-tail Fc. These results verified that FGF23 c-tail Fc counteracts FGF23 function at a known target *in vivo*, and provided mechanistic evidence of appropriate target engagement.

Normal serum levels of 1,25D and calcium are found following treatment with the murine FGF23 c-tail Fc

1,25D levels are normally increased by hypophosphatemia via increased expression of 1αOH (CYP27B1) expression in the kidney (2). However, FGF23 inhibits 1,25D by decreasing 1αOH expression. Thus, in Hyp animals, which have both high levels of FGF23 and hypophosphatemia, 1,25D levels are within the normal range. Inhibition of FGF23 using an anti-FGF23 antibody cocktail over a 4 week period in Hyp mice results in a strong increase in 1,25D levels 24 hrs post the final dose (17). Strikingly, in our study while minor statistically significant increases were seen upon treatment in 1,25D levels using trend p-value tests no significance was found using pairwise p-value analysis and overall the absolute levels were all very similar to those obtained in the C57BL/6J mice at the same timepoint. Therefore, as opposed to other molecules that inhibit the FGF23 pathway in the Hyp model, we found 1,25D levels did not change in a manner that would impact the biology with treatment at the 24hr time point (Figure 4A). In agreement with these findings, changes in CYP27B1 were not consistent across animals nor dose dependent (data not shown). In addition, this data is consistent with the lack of 1,25D modulation seen in the wild-type rat study, demonstrating that that the lack of 1,25D modulation spans species..

Inhibition of the FGF23 pathway in a similar model system has shown 1,25D elevation as early 5hrs post treatment and revealed that elevation can be sustained out to 7 days {Aono, 2009; Yamazaki, 2008}. In order to understand if 1,25D could be modulated by the FGF23 c-tail Fc at timepoints other than 24hrs we performed a single dose study in WT and Hyp animals (5 animals/grp) at 6hr and 72hr comparing 1,25D levels in animals treated with either vehicle or 15mg/kg FGF23 c-tail Fc. As shown in Supplementary Figure 1, the only change we were able to detect was in the Hyp mice at 6hrs and this change, though reaching significance, was less than 2 fold (285 vs 509 pg/ml) and was not sustained over time. As this response was transient and limited to the diseased state, we hypothesize that this movement may be due to the increase in phosphate which can feedback to effect 1,25D levels.

One function of 1,25D is to increase serum calcium levels by increasing uptake within the gut (2). As such, the increase of 1,25D seen after inhibition of FGF23 using an anti-FGF23 antibody cocktail in Hyp mice resulted in increased serum calcium (17). High levels of serum calcium increase the risk of soft tissue mineralization and therefore may indicate a safety risk. We assessed serum calcium levels in our Hyp study following the 7-week treatment. While calcium excretion was increased in a dose dependent manner upon treatment (Figure 4C), we found serum calcium to remain at normal levels following treatment with the FGF23 c-tail Fc (Figure 4B). As soft tissue mineralization is the

consequence of an elevated calcium/phosphate product, normal levels of 1,25D and calcium together with sub-normal levels of serum phosphate ensures a low risk of soft tissue mineralization. In agreement with this, no soft-tissue mineralization was observed in any animal group (data not shown).

FGF23 c-tail Fc treatment results in a significant improvement in cancellous bone and bone mineral content

Phosphate plays a major role in the mineralization of osteoid and cartilage at physes. In hypophosphatemic conditions such as XLH, this mineralization is compromised (1). We used several radiologic techniques to assess bone mineralization in treated and non-treated Hyp mice and compared these findings to those in untreated wild-type controls during our 7 week study.

PIXIMus is an automated densitometer used to measure Bone Mineral Density/Content in live animals, thereby allowing quantitative assessment of bone parameters. Consistent with published data (18–20), and relative to age-matched wild-type mice, Hyp mice displayed several skeletal abnormalities including: significantly lower bone mineral content (BMC), bone volume (BV) and bone mineral density (BMD) (Table 1). Together findings for these parameters strongly indicated poor bone mineralization that would eventually lead to compromised bone strength. Over the course of the study, treatment with 3mg/kg of FGF23 c-tail Fc showed a trend of improved BMC, BV and BMD, while treatment with 10mg/kg of FGF23 c-tail Fc produced significant improvement (Table 1). Importantly, individual animals within a group behaved similarly (Supplemental Figure 2). These data were consistent with increased modulation of clinical chemistries in the 10mg/kg treated animals and provided evidence for improved bone mineralization.

Improvement in bone mineralization and structure upon treatment of Hyp animals with 10mg/kg FGF23 c-tail Fc

To more directly assess bone quality we imaged the cancellous bone of the distal femoral metaphysis by performing *ex vivo* μCT. Cancellous bone is normally highly vascularized and metabolically active, and is therefore suitable for assessing remodeling. As expected, the wild-type control mice had far more cancellous bone at the distal femoral metaphysis than did the Hyp control animals. Remarkably, a clear dose responsive increase was seen after treatment. Because bone formation typically occurs at mechanically relevant bone areas, the increase in cancellous bone observed in our study was most evident at the proximal tibial metaphysis which transfers mechanical loads (Figure 5A).

To confirm the μCT, we performed intravital labeling of the newly mineralized bones by fluorescent labeling in a subset of animals. Specifically, mice were injected with calcein (green) and alizarin red (red) labels 10 and 3 days before the necropsy in order to assess active mineralization across animals of various backgrounds and treatment groups. As shown in Supplementary Figure 3, defined areas of cortical bone (femur) are labeled within WT mice while labeling in Hyp control mice is wide and fuzzy indicating diffuse mineralization patterns. Strikingly, both labels are much better defined in Hyp mice treated with 10 mg/kg/dose.

The poor bone quality of Hyp control animals was also evidenced by the large areas of scalloped bone surfaces, numerous pathological lacunae and open growth plates seen throughout the entire hock joint as visualized by three-dimensional μCT (Figure 5B). By day 50 of the study, growth plates had closed in the wild-type animals but remained open in the Hyp controls. Hyp mice treated with 10mg/kg of the FGF23 c-tail also showed normalization of bone surfaces characterized by absence of these pathological lacunae during our study (Figure 5B). In addition, closure of epiphyseal growth plates occurred after treatment with 10mg/kg of the FGF23 c-tail Fc (Figure 5B). Consistent with other data, Hyp mice in the 3 mg/kg group showed a moderate improvement; though the growth plates remained open in these animals.

Dose responsive improvement in bone histology evident upon treatment with FGF23 c-tail Fc

As a final assessment of FGF23 c-tail Fc impact on the bone, we performed histologic analysis of bone architecture at the proximal tibial physis of each animal. The physis is the part of the bone responsible for bone lengthening, constituting an area that separates the metaphysis and the epiphysis, in which long bone growth occurs. As seen in Figure 6, Hyp control animals not given FGF23 c-tail Fc had wide physes composed of cartilage. In contrast, the wild-type mice had thinner physes. Strikingly, there was marked improvement of the structure of physes in both treatment groups, with cartilage being replaced in a dose dependent manner by mineralized bone. Together these data demonstrate that the FGF23 c-tail treatment improved bone structure in Hyp animals during the 7 weeks of treatment.

Discussion

Current standard of care for XLH patients involves oral supplementation with phosphate and calcitrol, the active form of VitD (1). A major issue with the current treatment is achieving a balance between efficacy and unwanted toxicity. In the current study, we find that the FGF23 c-tail Fc selectively modulates the phosphate pathway without impacting 1,25D *in vivo* and ameliorates the bone defects present in Hyp mice, a mouse model that recapitulates XLH disease. We posit that the unique selectivity of the FGF23 c-tail Fc for the phosphate pathway provides efficacy together with a significant safety advantage, making it an improved therapeutic option in the chronic treatment of XLH.

A defining characteristic of untreated XLH is osteomalacia (1), the accumulation of unmineralized bone, a trait that is recapitulated in Hyp mice (18–20). Hyp mice have somewhat larger bones with significantly lower bone volume, BMC and BMD. Three-dimensional μCT images also showed large areas of scalloped bone surfaces, numerous lacunae throughout the hock joint and open growth plates in untreated Hyp animals, traits indicative of poor bone quality. Multiple doses of FGF23 c-tail Fc over our 7 week study produced significant improvement in bone mass as well as bone quality across the skeleton as measured by PIXIMUS. There was also a dose responsive improvement in bone surfaces, including diminished presence of pathological lacunae. At the highest dose of 10 mg/kg, growth plate closure occurred; growth plates remained open in the 3mg/kg group. Although significant improvement was observed, we noted that bone parameters were not normalized

by treatment. It remains to be determined if longer treatment or higher doses have the potential towould restore the skeletal properties of the cortical and cancellous bone to a greater degree.. Regardless, based on μCT, hematoxylin and eosin staining and intravital labeling our data indicate that multiple doses of FGF23 c-tail Fc resulted in substantial improvement in bone quality and reversed several aspects of disease similar to those which occur in XLH patients.

Interestingly, even in the presence of significant bone improvement only a moderate increase in serum phosphate at the highest treatment dose of 10mg/kg was achieved. In contrast, we found a dose responsive improvement in phosphate excretion that was normalized at the highest dose. The discrepancy in the magnitude of change between serum and excreted phosphate was somewhat surprising. The mechanism of action was verified because NaPi2A expression increased in a dose dependent manner after treatment. In the pathologic states with low NaPi expression, phosphate excretion is typically high. Thus, altering NaPi receptor levels causes an immediate block to phosphate excretion, making phosphate excretion the most proximal readout of this mechanism of action. A likely explanation for why the C-tail fails to normalize the serum phosphate may be that increased phosphate ions are consumed rapidly by the phosphate-deficient bone, thus preventing detection of sustained serum phosphorus increases. This may explain why the 3mg/kg dosed Hyp mice showed only a partial bone improvement despite a lack of a discernible increase in serum phosphate. If this occurs as bone mineralization occurs, serum phosphate may be expected to rise over time. Indeed, patients often experience a spike in serum phosphates when the requirement of phosphate in the bone changes (because of healing or changes in growth rates). The sub-normal levels of serum phosphate together with normal serum calcium levels provide a buffer for these potential spikes, limiting the chance of soft tissue mineralization in chronic therapy.

Several pre-clinical studies have explored the use of small molecule inhibitors and antibodies that target the FGF23 pathway for the treatment of XLH, using the Hyp mouse model (13, 17, 21). In each case, FGF23 signaling is inhibited and improvement of both hypophosphatemia and bone integrity is achieved. This is achieved through a variety of mechanisms including: pan inhibition of FGFRs (21), inhibition of the MAPK pathway (13) and neutralization of FGF23 itself (17). In each case, both phosphate and 1,25D levels are modulated. In the case of FGF23 neutralization, 1,25D modulation was sustained in a multi-dose 4 week study to levels approximately ten times over wild type levels (17). Consistent with the fact that 1,25D increases both calcium and phosphate absorption in the gut, serum levels of both analytes were significantly elevated in that study. Of note, at the dose that was efficacious for bone, the calcium phosphate solubility product in that study was indicative of soft-tissue mineralization. Though soft tissue mineralization was not seen in these animals, the risk present following 4 weeks of chronic dosing suggests this toxicity would be present if the study had been extended. Additionally, the presence of excess mineralization of metaphyseal cancellous bone within the treated Hyp mice suggests that the bone was saturated for phosphate.

In contrast, our FGF23 c-tail Fc showed selective inhibition of the phosphate pathway with an absence of biologically significant 1,25D modulation. We do not yet understand the

mechanism behind the preferential inhibition but speculate that it may be a consequence of antagonizing binding across several different receptor complexes, which in turn have different contributions in regulating the phosphate and 1,25D pathways. Indeed, genetic data have demonstrated unique requirements for individual FGFR/α-klotho receptor complexes in the regulation of phosphate and 1,25D (4, 23–26). Specifically, FGFR1c/α-klotho has been shown to be the primary receptor complex responsible for mediating phosphate (4) while there is a redundant requirement for FGFR3c/α-klotho and FGFR4/α-klotho in the control of 1,25D levels (24 2011). As the binding structure of FGF23 or the FGF23 c-tail to any of the FGFR/klotho complexes remains to be defined, it is difficult to predict how the c-tail may differentially interact across these receptors, and if it does act differently, whether this is at the level of binding or function. Intriguingly, preliminary data suggests that the FGF23 c-tail Fc fusion has unique competitive binding attributes across distinct receptor complexes as compared to that of the c-tail peptide. We remain actively engaged in exploring these possibilities.

While the mechanism mediating selective modulation remains to be determined, regulation of the phosphate pathway in the absence of 1,25D modulation was a result found in both wild-type and diseased animals in our study. Importantly in the XLH-disease model, improved bone integrity was also achieved. Interestingly, ectopic calcifications that are found in *Fgf23* null mice are no longer seen when these animals are crossed onto a 1α(OH) deficient background (27). This supports the idea that 1,25D is responsible for driving this toxicity in both the standard of care and *in vivo* studies where FGF23 is neutralized. We posit that the FGF23 c-tail Fc offers a potential safety advantage in the chronic treatment of XLH patients because it selectively modulates the phosphate pathway in the absence of 1,25D regulation and suggest it may be a new therapy for the treatment of both pediatric and adult XLH patients. An important next step for testing this hypothesis will be to assess the translation of our pre-clinical data to humans. It is interesting to think that nature has evolved to allow for the separate control of the phosphate and 1,25D pathways via the distinct action of the FGF23 c-tail. In healthy individuals, fluctuations in phosphate levels can be controlled via the processing of FGF23 whereas 1,25D levels can remain to be appropriately regulated by full length FGF23. We seek to harness the same properties in the chronic treatment of XLH.

Supplementary Material

Refer to Web version on PubMed Central for supplementary material.

Acknowledgments

The Mohammadi lab is primarily supported by the NIH grant DE13686. The work related to this manuscript was funded by Pfizer Inc. Centers for Therapeutic Innovation. We would like to thank Carolyn Macica, Mohammed Razzaque and CTI team members for helpful discussions. We would like to thank Carol Fritz and other Biomarker team members for serum and urine chemistry analyses.

References

1. Carpenter TO, Imel EA, Holm IA, Jan de Beur SM, Insogna KL. A clinician's guide to X-linked hypophosphatemia. J Bone Miner Res. 2011; 26(7):1381–8. [PubMed: 21538511]

2. Bergwitz C, Juppner H. Regulation of phosphate homeostasis by PTH, vitamin D, and FGF23. Annu Rev Med. 2010; 61:91–104. [PubMed: 20059333]

3. Shimada T, Urakawa I, Yamazaki Y, Hasegawa H, Hino R, Yoneya T, et al. FGF-23 transgenic mice demonstrate hypophosphatemic rickets with reduced expression of sodium phosphate cotransporter type IIa. Biochem Biophys Res Commun. 2004; 314(2):409–14. [PubMed: 14733920]

4. Gattineni J, Bates C, Twombley K, Dwarakanath V, Robinson ML, Goetz R, et al. FGF23 decreases renal NaPi-2a and NaPi-2c expression and induces hypophosphatemia in vivo predominantly via FGF receptor 1. Am J Physiol Renal Physiol. 2009; 297(2):F282–91. [PubMed: 19515808]

5. Larsson T, Marsell R, Schipani E, Ohlsson C, Ljunggren O, Tenenhouse HS, et al. Transgenic mice expressing fibroblast growth factor 23 under the control of the alpha1(I) collagen promoter exhibit growth retardation, osteomalacia, and disturbed phosphate homeostasis. Endocrinology. 2004; 145(7):3087–94. [PubMed: 14988389]

6. Bai XY, Miao D, Goltzman D, Karaplis AC. The autosomal dominant hypophosphatemic rickets R176Q mutation in fibroblast growth factor 23 resists proteolytic cleavage and enhances in vivo biological potency. J Biol Chem. 2003; 278(11):9843–9. [PubMed: 12519781]

7. Bai X, Miao D, Li J, Goltzman D, Karaplis AC. Transgenic mice overexpressing human fibroblast growth factor 23 (R176Q) delineate a putative role for parathyroid hormone in renal phosphate wasting disorders. Endocrinology. 2004; 145(11):5269–79. [PubMed: 15284207]

8. Shimada T, Hasegawa H, Yamazaki Y, Muto T, Hino R, Takeuchi Y, et al. FGF-23 is a potent regulator of vitamin D metabolism and phosphate homeostasis. J Bone Miner Res. 2004; 19(3):429–35. [PubMed: 15040831]

9. Shimada T, Muto T, Urakawa I, Yoneya T, Yamazaki Y, Okawa K, et al. Mutant FGF-23 responsible for autosomal dominant hypophosphatemic rickets is resistant to proteolytic cleavage and causes hypophosphatemia in vivo. Endocrinology. 2002; 143(8):3179–82. [PubMed: 12130585]

10. White KE, Carn G, Lorenz-Depiereux B, Benet-Pages A, Strom TM, Econs MJ. Autosomal-dominant hypophosphatemic rickets (ADHR) mutations stabilize FGF-23. Kidney Int. 2001; 60(6):2079–86. [PubMed: 11737582]

11. Goetz R, Beenken A, Ibrahimi OA, Kalinina J, Olsen SK, Eliseenkova AV, et al. Molecular insights into the klotho-dependent, endocrine mode of action of fibroblast growth factor 19 subfamily members. Mol Cell Biol. 2007; 27(9):3417–28. [PubMed: 17339340]

12. Goetz R, Nakada Y, Hu MC, Kurosu H, Wang L, Nakatani T, et al. Isolated C-terminal tail of FGF23 alleviates hypophosphatemia by inhibiting FGF23-FGFR-Klotho complex formation. Proc Natl Acad Sci U S A. 2010; 107(1):407–12. [PubMed: 19966287]

13. Zhang MY, Ranch D, Pereira RC, Armbrecht HJ, Portale AA, Perwad F. Chronic inhibition of ERK1/2 signaling improves disordered bone and mineral metabolism in hypophosphatemic (Hyp) mice. Endocrinology. 2012; 153(4):1806–16. [PubMed: 22334725]

14. Goetz R, Ohnishi M, Kir S, Kurosu H, Wang L, Pastor J, et al. Conversion of a paracrine fibroblast growth factor into an endocrine fibroblast growth factor. J Biol Chem. 2012; 287(34):29134–46. [PubMed: 22733815]

15. Sitara D, Razzaque MS, Hesse M, Yoganathan S, Taguchi T, Erben RG, et al. Homozygous ablation of fibroblast growth factor-23 results in hyperphosphatemia and impaired skeletogenesis, and reverses hypophosphatemia in Phex-deficient mice. Matrix Biol. 2004; 23(7):421–32. [PubMed: 15579309]

16. Liu S, Zhou J, Tang W, Jiang X, Rowe DW, Quarles LD. Pathogenic role of Fgf23 in Hyp mice. Am J Physiol Endocrinol Metab. 2006; 291(1):E38–49. [PubMed: 16449303]

17. Aono Y, Yamazaki Y, Yasutake J, Kawata T, Hasegawa H, Urakawa I, et al. Therapeutic effects of anti-FGF23 antibodies in hypophosphatemic rickets/osteomalacia. J Bone Miner Res. 2009; 24(11):1879–88. [PubMed: 19419316]

18. Eicher EM, Southard JL, Scriver CR, Glorieux FH. Hypophosphatemia: mouse model for human familial hypophosphatemic (vitamin D-resistant) rickets. Proc Natl Acad Sci U S A. 1976; 73(12): 4667–71. [PubMed: 188049]

19. Meyer RA Jr, Gray RW, Meyer MH. Abnormal vitamin D metabolism in the X-linked hypophosphatemic mouse. Endocrinology. 1980; 107(5):1577–81. [PubMed: 6893581]

20. Delvin EE, Glorieux FH. Serum 1,25-dihydroxyvitamin D concentration in hypophosphatemic vitamin D-resistant rickets. Calcif Tissue Int. 1981; 33(2):173–5. [PubMed: 6260313]

21. Wohrle S, Henninger C, Bonny O, Thuery A, Beluch N, Hynes NE, et al. Pharmacological inhibition of fibroblast growth factor (FGF) receptor signaling ameliorates FGF23-mediated hypophosphatemic rickets. J Bone Miner Res. 2013; 28(4):899–911. [PubMed: 23129509]

22. Shalhoub V, Shatzen EM, Ward SC, Davis J, Stevens J, Bi V, et al. FGF23 neutralization improves chronic kidney disease-associated hyperparathyroidism yet increases mortality. J Clin Invest. 2012; 122(7):2543–53. [PubMed: 22728934]

23. Li H, Martin A, David V, Quarles LD. Compound deletion of Fgfr3 and Fgfr4 partially rescues the Hyp mouse phenotype. Am J Physiol Endocrinol Metab. 2011; 300(3):E508–17. [PubMed: 21139072]

24. Gattineni J, Twombley K, Goetz R, Mohammadi M, Baum M. Regulation of serum 1,25(OH)2 vitamin D3 levels by fibroblast growth factor 23 is mediated by FGF receptors 3 and 4. Am J Physiol Renal Physiol. 2011; 301(2):F371–7. [PubMed: 21561999]

25. Kurosu H, Ogawa Y, Miyoshi M, Yamamoto M, Nandi A, Rosenblatt KP, et al. Regulation of fibroblast growth factor-23 signaling by klotho. J Biol Chem. 2006; 281(10):6120–3. [PubMed: 16436388]

26. Urakawa I, Yamazaki Y, Shimada T, Iijima K, Hasegawa H, Okawa K, et al. Klotho converts canonical FGF receptor into a specific receptor for FGF23. Nature. 2006; 444(7120):770–4. [PubMed: 17086194]

27. Sitara D, Razzaque MS, St-Arnaud R, Huang W, Taguchi T, Erben RG, et al. Genetic ablation of vitamin D activation pathway reverses biochemical and skeletal anomalies in Fgf-23-null animals. Am J Pathol. 2006; 169(6):2161–70. [PubMed: 17148678]

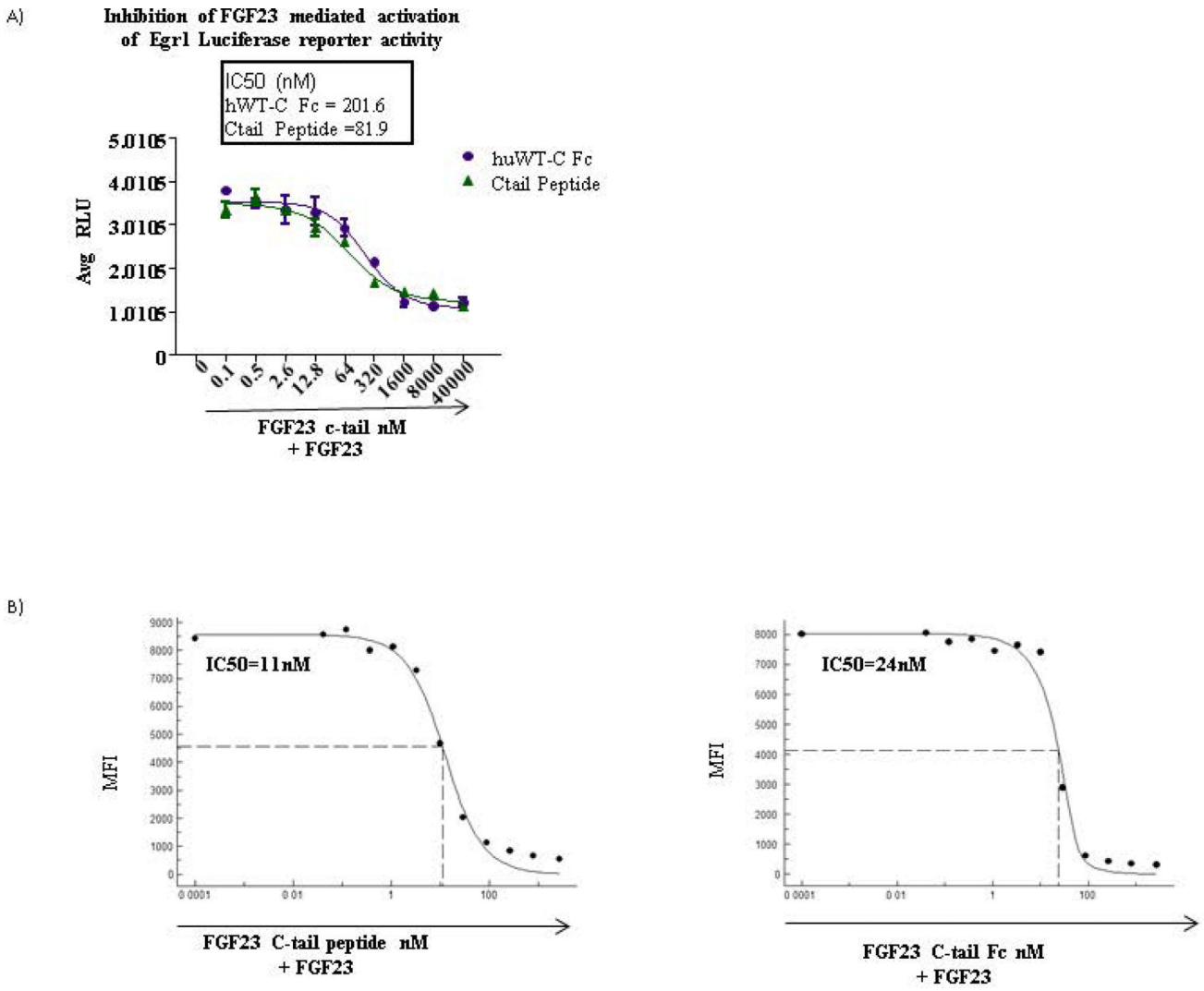

Figure 1. Human 72aa FGF23 C-tail Fc fusion has an inhibitory potency similar to the human 72aa FGF23 C-tail peptide

(A) IC50s derived for both the FGF23 c-tail peptide and Fc fusion based on luciferase activity from a HEK293-klotho-Egr1 reporter cell line using increasing amounts of either FGF23 c-tail peptide or FGF23 c-tail Fc prior to stimulating cells with sub-saturating amounts of recombinant FGF23 (B) IC50s derived from competitive binding assessment in HEK293-klotho lines using the MFI from individual samples of increasing amounts of either FGF23 c-tail peptide or Fc followed by binding of sub-saturating amounts of FGF23. Data representative of n=3.

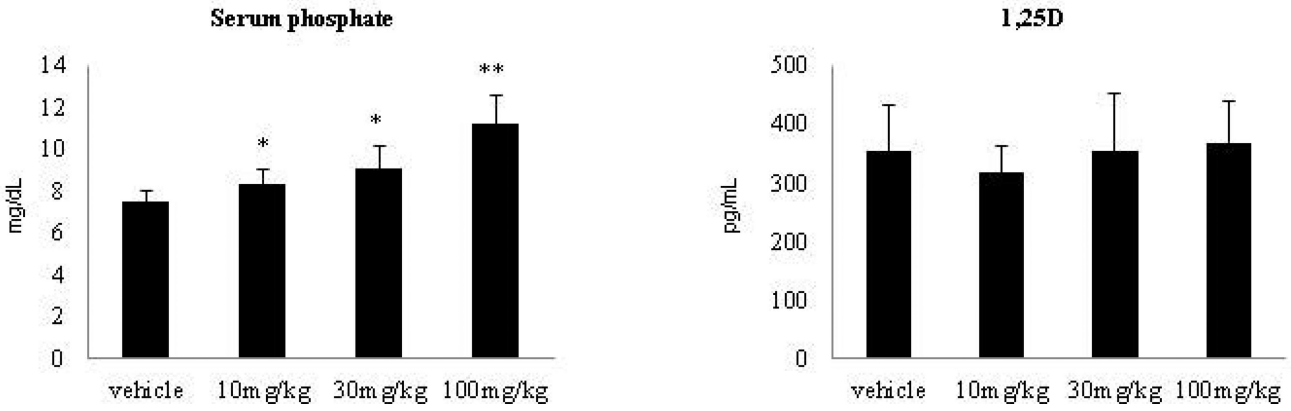

Figure 2. FGF23 C-tail Fc modulates serum phosphate but not 1,25D in wild-type rats

Serum chemistry analysis performed 24 hrs post the 5th dose in wild-type rats. Data represents averages of 5 rats. * Significantly different from vehicle control $p<0.05$; ** significantly different from vehicle control $p<0.01$

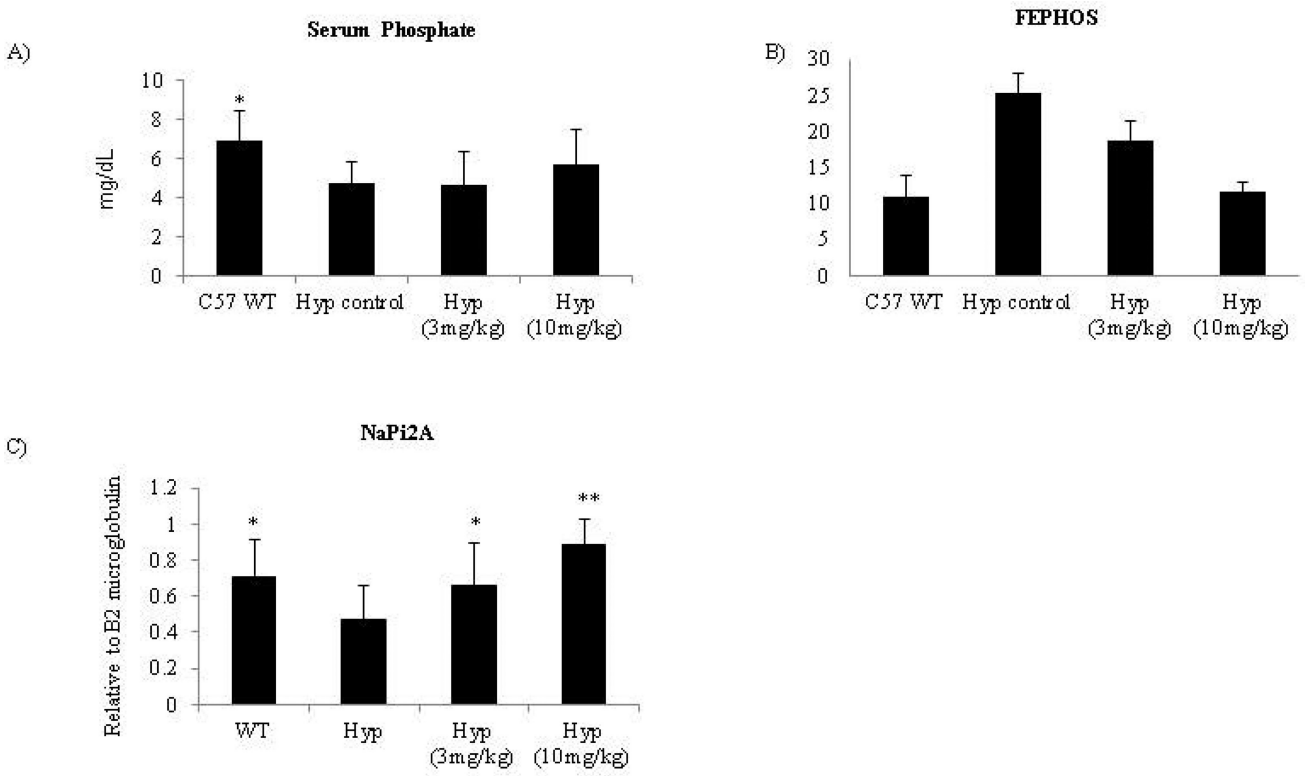

Figure 3. Murine FGF23 c-tail Fc modulates phosphate levels in Hyp mice via regulation of NaPi2A expression

(A) Serum phosphate values are the averages of 10 mice/grp 24hrs post final dose on D52 and (B) FEPHOSH (ratio of: serum creatinine/serum phosphorus / urine creatinine/urine phosphate) values are the average of serumserum chemistry parameters from10 mice/grp 24hrs post final dose on D52; urine data represents 2 grps of pooled urine from 5 animals/ group with collection occurring 12–24hrs post final dosing in non-fasted animals. The necessity to pool urine samples resulted in 2 data points/10 animals and thus prohibited statistical analysis of FEPHOSH. (C) NaPi2A expression relative to B2 microglobulin was assessed from total kidney RNA 24hrs post the final dose on D52 via QPCR. Data represents the average of 10 mice/group. * Significantly different from Hyp control $p<0.05$; ** Significantly different from Hyp control $p<0.01$

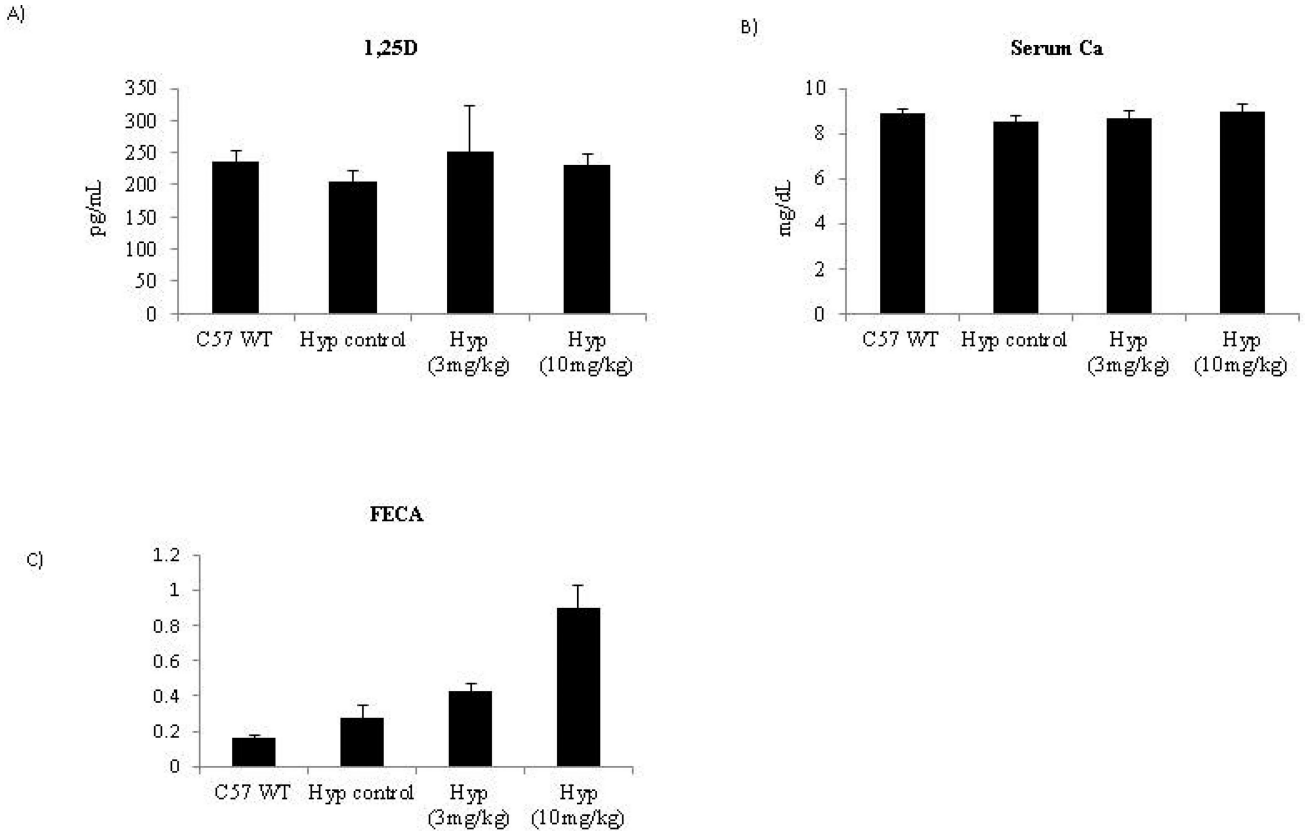

Figure 4. Normal serum levels of 1,25D and calcium are found following treatment with the murine FGF23 c-tail Fc

(A) Serum 1,25D values are the averages of 10 mice/grp 24hrs post final dose on D52 and (B) serum calcium values are the average of 10 mice/grp 24hrs post final dose on D52. (C) FECA values (ratio of: serum creatinine/serum calcium over urine creatinine/urine calcium) are the average of serum chemistry parameters from 10 mice/grp 24hrs post final dose on D52; urine data represents 2 grps of pooled urine from 5 animals/group with collection occurring 12–24hrs post final dosing in non-fasted animals. The necessity to pool urine samples prohibited statistical analysis of FECA.

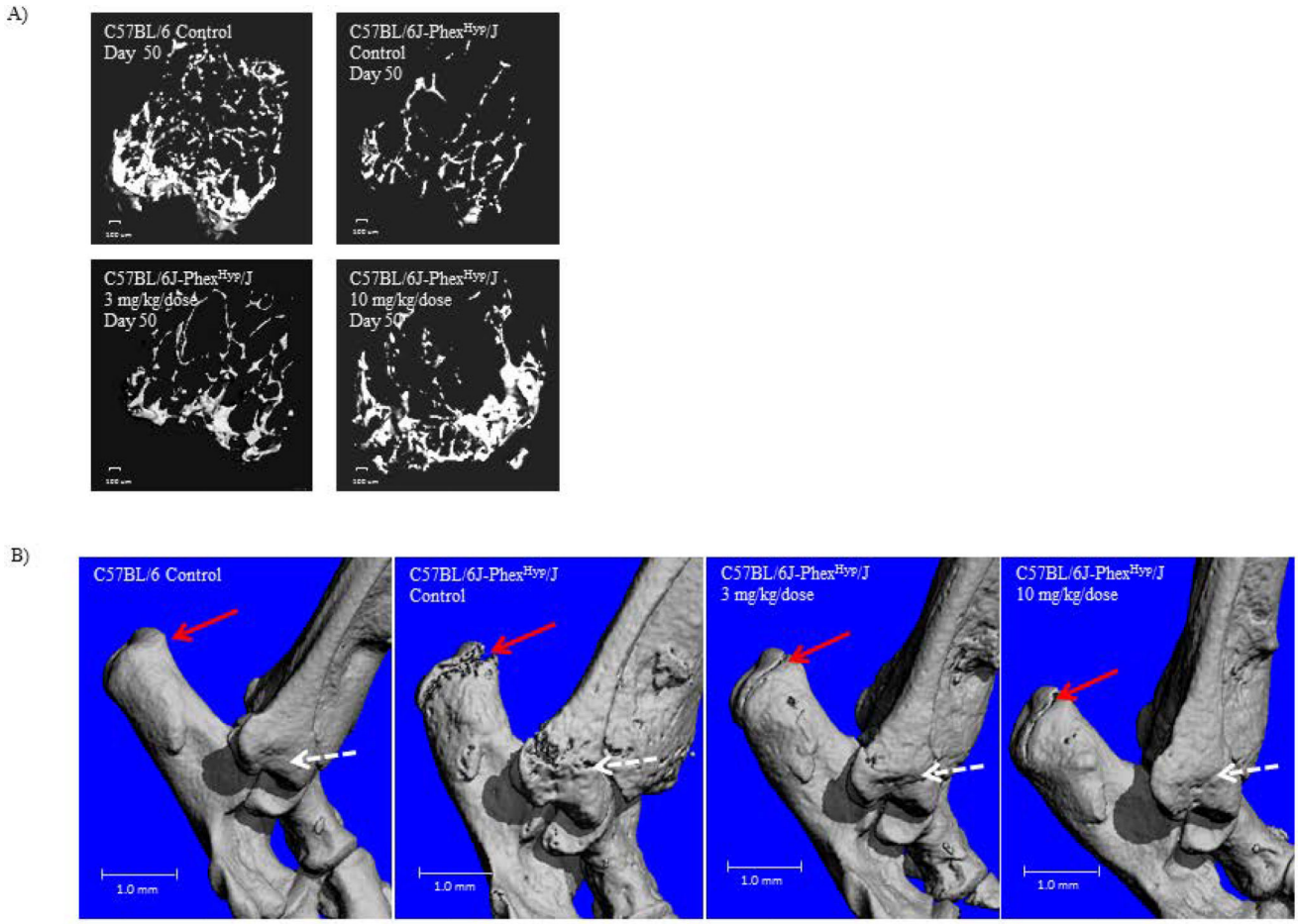

Figure 5. Improvement in bone mineralization and structure upon treatment of Hyp animals with 10mg/kg FGF23 c-tail Fc

(A) Visualization of the cancellous bone of the distal femoral metaphysis as imaged by *ex vivo* μCT. A 100μm scale bar is indicated. (B) Depiction of bone quality as imaged via three-dimensional space filling analysis using μCT. For both these measures, these μCT images are representative of those in the following groups: C57BL/6 Control (n=10 mice); C57BL/6J-PhexHyp/J Control (n=10 mice); C57BL/6J-PhexHyp/J 3 mg/kg/dose (n=10 mice); C57BL/6J-PhexHyp/J 10 mg/kg/dose (n=10 mice). A 1mm scale bar is indicated.

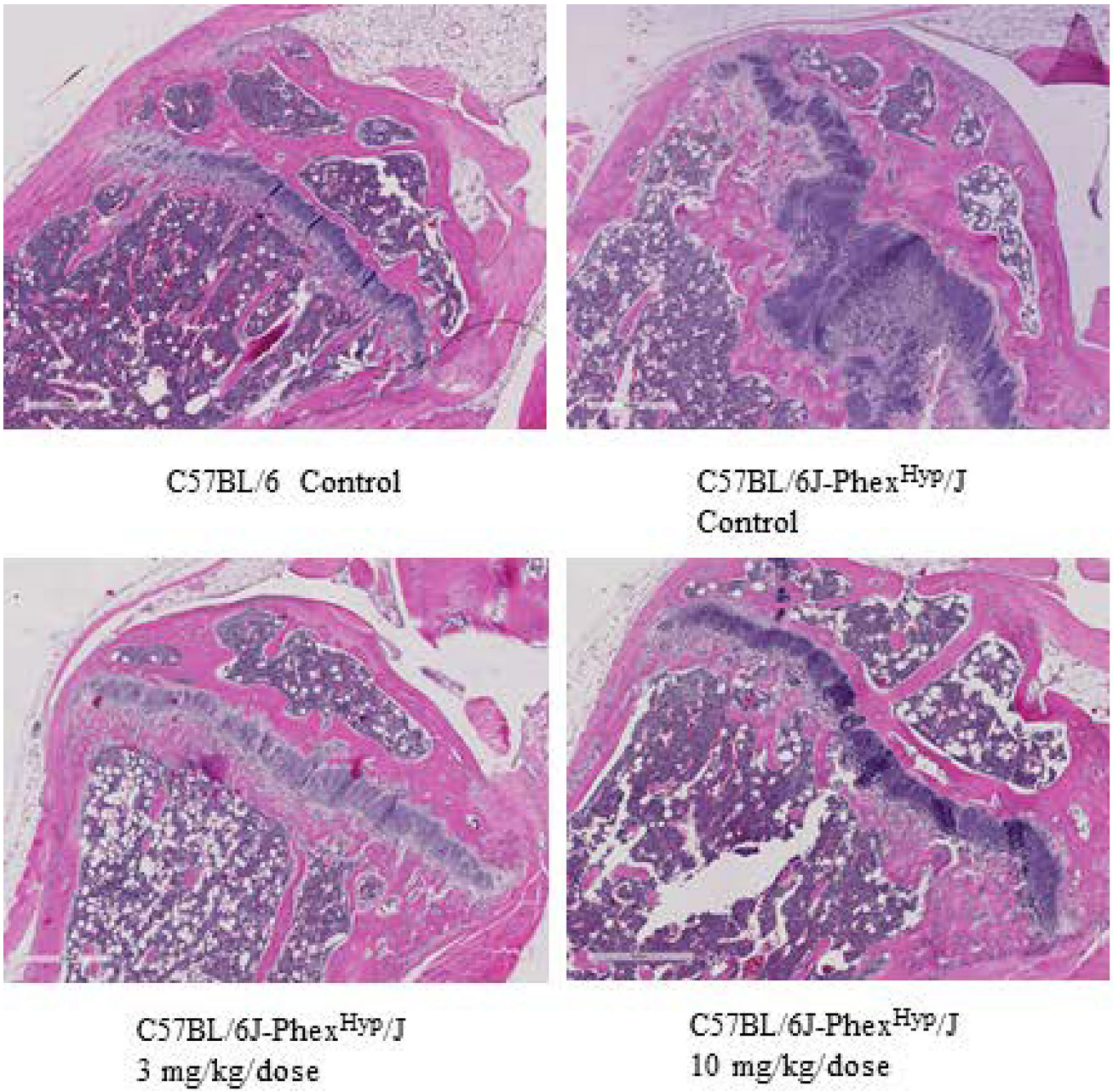

Figure 6. Dose responsive improvement in bone architecture is evident upon treatment with FGF23 c-tail Fc

Hematoxylin and eosin staining of tibial physes depicts bone architecture. Images are representative of microscopic findings in the following groups: C57BL/6 Control (n=10 mice); C57BL/6J-PhexHyp/J Control (n=10 mice); C57BL/6J-PhexHyp/J 3 mg/kg/dose (n=10 mice); C57BL/6J-PhexHyp/J 10 mg/kg/dose (n=10 mice). A scale bar of 400 microns is included within each image.

Table 1

Mean values (± SD) for measurements of the bone parameters in mice on Day 50.

		C57BL/6J	C57BL/6J-Phex^{Hyp}/J		
Parameter	**Unit**	**Control (Group 1)**	**Control (Group 2)**	**3 mg/kg/dose (Group 3)**	**10 mg/kg/dose (Group 4)**
BMD	gm/cm^2	0.045 ± 0.001	0.036 ± 0.002[1]	0.039 ± 0.002[a]	0.040 ± 0.002[a]
BMC	gm	0.42 ± 0.026	028 ± 0.019[1]	0.32 ± 0.031[a]	0.33 ± 0.028[a]
BMA	cm^2	9.35 ± 0.660	7.75 ± 0.218[1]	8.21 ± 0.576	8.28 ± 0.799

[1] Significantly different form C57BL/6J control, $p \leq 0.01$;

[a] Significantly different form C57BL/6J-Phex^{Hyp}/J control, $p \leq 0.01$